


Article

Application of MLR, BP and PCA-BP Neural Network for Predicting FeO in Bottom-Blowing O₂-CaO Converter

Xin Ren ^{1,2} , Kai Dong ^{1,2,*}, Chao Feng ^{1,2,*}, Rong Zhu ^{1,2}, Guangsheng Wei ^{1,2} and Chunyang Wang ^{1,2}

¹ School of Metallurgical and Ecological Engineering, University of Science and Technology Beijing, Beijing 100083, China; renxin1108@163.com (X.R.); zrongustb@163.com (R.Z.); wgshsteel@126.com (G.W.); 17801055109@163.com (C.W.)

² Beijing Key Laboratory of Research Center of Special Melting and Preparation of High-end Metal Materials, University of Science and Technology Beijing, Beijing 100083, China

* Correspondence: dkaiustb@163.com (K.D.); ustbfengchao@163.com (C.F.)

Abstract: In order to accurately predict the FeO content of slag in the bottom-blowing O₂-CaO process of the dephosphorization converter, multiple linear regression model, backpropagation (BP) neural network model and principal component analysis–backpropagation (PCA-BP) combined with neural network model were established to predict the FeO content of slag. It was found that the PCA-BP combined neural network model has the highest prediction accuracy by using principal component analysis to reduce the dimension of influencing factors of FeO content in slag and eliminate the correlation between input variables. The average absolute error is 1.178%, which is 0.78% lower than that of multiple linear regression model and 0.453% lower than that of multiple linear regression model. When the prediction error range is 3.0%, the prediction hit rate of the model is 96%, and when the prediction error range is 2.0%, the prediction hit rate of the model is 78%. The prediction model has important reference value for actual production.

Keywords: converter; bottom-blowing O₂-CaO process; FeO prediction; multiple linear regression; BP neural network; PCA-BP combined neural network



Citation: Ren, X.; Dong, K.; Feng, C.; Zhu, R.; Wei, G.; Wang, C.

Application of MLR, BP and PCA-BP Neural Network for Predicting FeO in Bottom-Blowing O₂-CaO Converter. *Metals* **2023**, *13*, 782. <https://doi.org/10.3390/met13040782>

Academic Editors: Alexander McLean and Pasquale Cavaliere

Received: 12 February 2023

Revised: 22 March 2023

Accepted: 7 April 2023

Published: 16 April 2023



Copyright: © 2023 by the authors. Licensee MDPI, Basel, Switzerland. This article is an open access article distributed under the terms and conditions of the Creative Commons Attribution (CC BY) license (<https://creativecommons.org/licenses/by/4.0/>).

1. Introduction

With the continuous improvement of and demand for the social high-quality development of quality steel materials, the deep removal of phosphorus has increasingly become a technical problem in the production of high-quality steel products [1]. Except for a few special steel grades, such as weathering steel and cannonball steel, phosphorus is a harmful element for most steel grades. Although phosphorus can increase the strength and hardness of steel, it can significantly reduce the plasticity and impact toughness. Especially at a low temperature, it makes steel become obviously brittle, which is called “cold brittleness”. Cold brittleness deteriorates the cold working and weldability of steel. The higher the phosphorus content, the greater the cold brittleness, so the phosphorus content in steel is strictly controlled [2,3].

As the main raw material for converter dephosphorization, the dissolution rate of lime in the converter directly affects the dephosphorization capacity of converter slag [4]. The rapid dissolution of lime can timely form slag with good fluidity and appropriate alkalinity, thus providing favorable thermodynamic and dynamic conditions for converter dephosphorization and realizing the efficient dephosphorization of molten steel. A high FeO content in slag can promote lime dissolution. Deng [5] believes that FeO in lime and slag can penetrate between the 2CaO·SiO₂ shell and CaO shell, forming a rich FeO layer and weakening the conditions for lime surface to adsorb the 2CaO·SiO₂ shell, and then the 2CaO·SiO₂ shell can be opened through slag movement, thus playing a role in shell breaking.

In order to achieve a better dephosphorization effect, this team of researchers successfully carried out the industrial test of bottom-blowing O_2 -CaO in a 300 t dephosphorization converter of a steel plant. All the lime needed for dephosphorization can be directly sprayed into the molten pool from the bottom in the form of powder, which can obtain a larger dephosphorization reaction interface and a higher stirring intensity in the molten pool [6]. The bottom-blowing O_2 -CaO process in a converter takes oxygen as the carrier gas of lime powder, which has good thermodynamic conditions for dephosphorization, and the phosphorus distribution ratio can reach 2–4 times that of a conventional converter. It can reduce the consumption of raw and auxiliary materials for steelmaking and obtain an excellent dephosphorization effect. However, during the test, it was found that, compared with the conventional converter process, the bottom-blowing O_2 -CaO process greatly reduced the FeO content in the slag. The drastic reduction of FeO in slag will inevitably affect the utilization rate of lime and the judgment of the oxidation at the end of the molten pool, and then it will affect the oxygen supply system of the top lance of the converter and the design of the bottom-blowing curve. Therefore, in the process of converter steelmaking, if the end FeO content can be accurately predicted, it will have guiding significance for the optimization of the converter bottom-blowing O_2 -CaO process.

In order to predict the endpoint FeO content of slag, Akitoshi Matsuyi et al. [7] established a dynamic model of FeO formation in molten iron and, based on this, established a dynamic mathematical model of dephosphorization in molten iron, and estimated the endpoint FeO content. The error between the predicted value and the measured value is within 5%, so dephosphorization can be controlled through the prediction of FeO. Zhao [8] established a prediction model of FeO in slag combined with the field production data by using the oxygen balance theory in the material balance calculation. The model can also be used to calculate the relationship between FeO content in slag, top-blown oxygen content and slag phosphorus ratio. The verification results show that the FeO content of slag calculated by the model is in good agreement with the measured value, and the proportion of absolute error within 5% and relative error within 10% is over 80%.

The above slag FeO prediction methods mainly rely on the mechanism model. However, there are complex physical and chemical reactions, heat and mass transfer and multiphase flow characteristics in the converter. In addition, under the closed conditions of high temperature, high pressure, and multiphase and multifield coupling, solid–liquid–gas polymorphisms coexist. Therefore, in actual production practice, it is difficult to achieve more accurate prediction results by using the above model. At the same time, due to the development of detection means, it is difficult to directly detect the slag composition online, and the offline assay time lag is long.

Therefore, based on the production data of the 300 t dephosphorization converter bottom-blowing O_2 -CaO process in a steel plant, this paper attempts to establish a prediction model of FeO content in slag under bottom-blowing O_2 -CaO process by means of statistical learning technology and artificial intelligence technology. In this paper, a multiple linear regression prediction model [9,10], BP neural network prediction model and PCA-BP combined neural network prediction model [11,12] are established to predict the slag FeO content of converter bottom-blowing O_2 -CaO process, and the three models are simulated, which provide a basis for optimizing the operating system of converter bottom-blowing O_2 -CaO process and a new way for metallurgical prediction modeling.

2. Industrial Test and Data Collection

2.1. Test Device

Figure 1 shows the schematic diagram of converter bottom-blowing O_2 -CaO process, including the feeding system, injection system and smelting system. The lime required for smelting can be sprayed from the bottom of the converter in the form of powder. The maximum powder injection flow is designed to be $240 \text{ kg}\cdot\text{min}^{-1}$, and the equivalent powder injection intensity is $0.8 \text{ kg}\cdot\text{t}^{-1}\cdot\text{min}^{-1}$, meeting the lime demand of the dephosphorization furnace. The carrier gas for bottom blowing is an O_2 - CO_2 mixture or O_2 - N_2 mixture.

The flow of carrier gas is $2700 \text{ Nm}^3 \cdot \text{h}^{-1}$, and the bottom-blowing intensity can reach $0.2 \text{ Nm}^3 \cdot \text{t}^{-1} \cdot \text{min}^{-1}$. The process and equipment parameters of lime powder injection at the bottom of the dephosphorization converter are shown in Table 1.

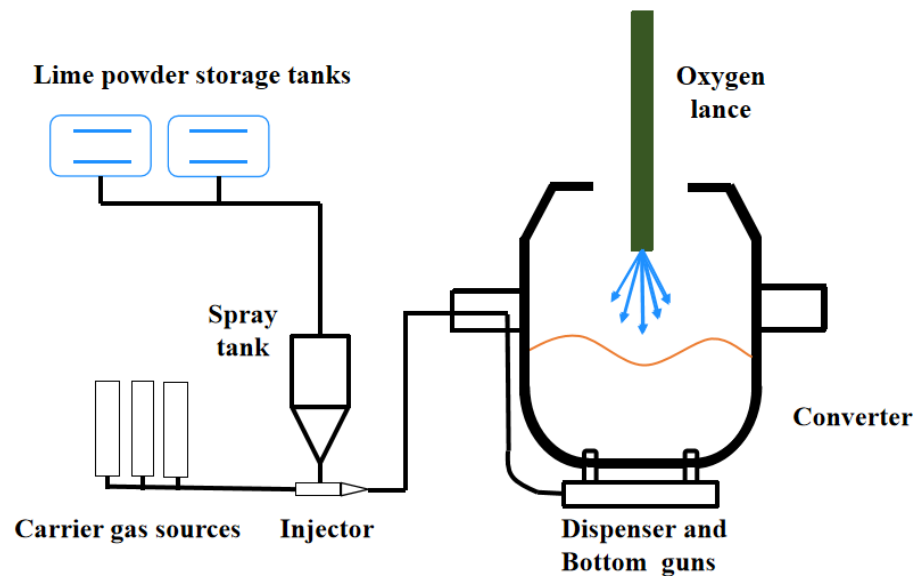


Figure 1. Schematic diagram of converter bottom-blowing $\text{O}_2\text{-CaO}$ process.

Table 1. Parameters of bottom-blowing $\text{O}_2\text{-CaO}$ process in 300 t dephosphorization converter.

Parameter	Value	Parameter	Value
Nominal capacity of converter	300t	Weight of powder injection per heat	2000–4000 kg
Number of bottom-blowing guns	2	Type of carrier gas	$\text{O}_2/\text{CO}_2/\text{N}_2/\text{Ar}$
Total flow rate of bottom carrier gas	$2700 \text{ Nm}^3/\text{h}$	Bottom-blowing powder flow rate	0–240 kg/min

2.2. FeO Content in Slag of Conventional/Bottom-Blowing $\text{O}_2\text{-CaO}$ Process

The production data of the 300t dephosphorization converter conventional process and bottom-blowing $\text{O}_2\text{-CaO}$ process in a steel plant are selected, and the FeO content in the slag of the two processes is shown in Figure 2. It can be seen from Figure 2 that the average endpoint FeO content of slag in the traditional process is 31.14%, and the fluctuation range is large, with a minimum value of 10% and a maximum value of about 47%. The average FeO content in the slag of the $\text{O}_2\text{-CaO}$ bottom-blowing process is 12.15%, which is relatively concentrated; and it is nearly 20% lower than that of conventional process.

It can be seen that the converter bottom-blowing $\text{O}_2\text{-CaO}$ process has subversive changes in slag composition, especially FeO content, compared with the conventional process, resulting in fundamental changes in a series of operating systems, such as the auxiliary material loading system and oxygen supply system. Therefore, it is necessary to predict the FeO content of the converter bottom-blowing $\text{O}_2\text{-CaO}$ process, so as to effectively guide actual production.

2.3. Data Collection and Filtering

Since the multiple linear regression analysis and BP neural network learning are based on a large number of production data, the author collected 342 production data of the industrial test of the bottom-blowing $\text{O}_2\text{-CaO}$ process in a 300 t dephosphorization converter in a steel plant. After removing abnormal heats and some numerical default heats, 267 valid production data were obtained as prediction modeling samples. In order

to establish the prediction verification model, 217 heats of production data are used as the training set to model, and the remaining 50 heats of production data are used as the test set to verify the established prediction model.

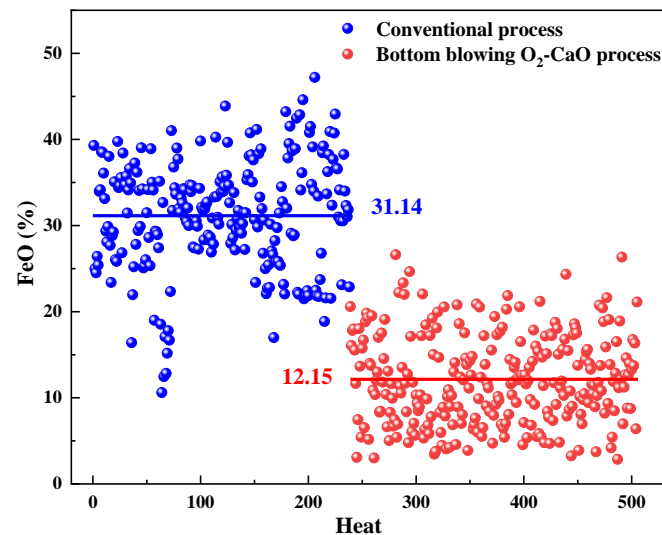


Figure 2. Comparison of FeO content in slag of conventional process and bottom-blowing O₂-CaO process.

To establish a high-precision prediction model, the selection of input parameters is very important. In order to accurately predict the FeO content of slag, the parameters in the production report of 267 heats were preliminarily selected according to metallurgical knowledge. According to metallurgical theory and practical production practice, taking into account metallurgical reaction principles such as kinetics, thermodynamics and chemical balance and applying SPSS software (IBM Corporation, New York, NY, USA) for statistical screening and a correlation test, the input parameters of the prediction model of FeO in slag are finally determined: hot metal weight, hot metal temperature, hot metal [C] content, hot metal [Si] content, tapping temperature, endpoint [C] content, endpoint [Si] content, slag (CaO) content, slag basicity, dolomite weight, sinter weight, bottom-sprayed CaO weight, top-added CaO weight, top-blown O₂ consumption, bottom-blown O₂ consumption and bottom-blown N₂ consumption. The descriptive statistics of these parameters are obtained from actual production data, as shown in Table 2.

Table 2. Descriptive statistics of the process variables.

Variable	Symbol	Unit	Variable	Symbol	Unit
Hot metal weight	X ₁	t	Hot metal temperature	X ₂	°C
Hot metal [C] content	X ₃	%	Hot metal [Si] content	X ₄	%
Tapping temperature	X ₅	°C	Endpoint [C] content	X ₆	%
Endpoint [Si] content	X ₇	%	Slag (CaO) content	X ₈	°C
Slag basicity	X ₉	t	Dolomite weight	X ₁₀	t
Sinter weight	X ₁₁	t	Bottom-sprayed CaO weight	X ₁₂	t
Top-added CaO weight	X ₁₃	t	Top-blown O ₂ consumption	X ₁₄	Nm ³
Bottom-blown O ₂ consumption	X ₁₅	Nm ³	Bottom-blown N ₂ consumption	X ₁₆	Nm ³
FeO content	Y	%			

3. Prediction Model of FeO in Slag Based on MLR

The multiple regression model (MLR), which is a kind of algebraic model, is generally obtained by mathematical statistics; that is, the model is established through the collection, collation and statistical analysis of field data [13,14]. Under the stable production conditions

and public welfare operation mode, converter steelmaking has good reproducibility and repeatability. Therefore, this paper firstly makes multiple linear regression on the smelting data of the converter bottom-blowing O₂-CaO process and establishes a regression prediction model of the FeO content in the converter bottom-blowing O₂-CaO process.

3.1. Introduction and Establishment of MLR

In statistics, the multiple linear regression analysis is a statistical analysis method that is used to study the linear relationship between one dependent variable and several independent variables [15]. The FeO content in slag is affected by many factors, so, in theory, the multiple linear regression method can be used to analyze the relationship between the FeO content in slag and influencing factors, and a prediction model can be established. y is the dependent variable, and $x_1, x_2, x_3 \dots$ are the independent variables; the formula of the multiple linear regression model is Equation (1):

$$y_i = \beta_0 + \beta_1 \times x_1 + \beta_2 \times x_2 + \beta_3 \times x_3 + \dots + \beta_k \times x_k \quad (1)$$

where k is the number of explanatory variables, and β_j ($j = 1, 2, \dots, k$) is called the regression coefficient.

SPSS statistical analysis software is one of the most popular statistical software applications at present that is widely used in various fields of social science and natural science [16]. Based on this, the FeO content in slag and its influencing factors are modeled and analyzed by SPSS statistical analysis software. Sixteen independent variables established in the previous section are used as input variables of SPSS regression model, and the FeO content of slag is used as the output variables of the model.

The effective production data of 267 heats screened in the previous section are used as the prediction modeling sample. Among them, 217 heats of data are used as the training set to model, and the remaining 50 heats of data are used as a test set to verify the established prediction model.

3.2. Prediction Results and Test of Multiple Regression Prediction Model

SPSS software was used to carry out the regression analysis on the data of 217 heats of the converter bottom-blowing O₂-CaO process. The results are shown in Tables 3 and 4. According to Table 3, the regression equation $R^2 = 0.933 > 0.9$ indicates that the regression equation has a good fitting degree and that the performance of the model is good. The F value of the regression equation, $F = 173.439 > F_{\alpha}(16,200) = 21.69$, shows that the regression equation is significant and the regression effect is remarkable. The combination of 16 variables considered in the model has a significant impact on the FeO content in slag. The standard error of regression coefficient $\text{Sig.}, \text{Sig.} = 0.000 < 0.05$, shows that independent variables have significant influence on dependent variables. The regression coefficient passed the test; that is, the empirical formula between influencing factors and the FeO content of slag determined by multiple linear regression method is available. According to the results in Table 4, the established multiple linear regression equation is shown in Equation (2):

$$Y = -3.884 \times 10 + 1.061 \times 10^{-1} \cdot X_1 - 1.245 \times 10^{-2} \cdot X_2 - 1.491 \cdot X_3 + 2.355 \cdot X_4 - 1.055 \times 10^{-4} \cdot X_5 + 1.205 \cdot X_6 + 1.430 \times 10 \cdot X_7 - 1.726 \cdot X_8 + 1.522 \times 10 \cdot X_9 - 6.099 \times 10 \cdot X_{10} + 8.491 \times 10^{-2} \cdot X_{11} + 7.477 \times 10^{-1} \cdot X_{12} - 1.072 \times 10^{-2} \cdot X_{13} + 1.425 \times 10^{-3} \cdot X_{14} - 1.453 \times 10^{-2} \cdot X_{15} + 3.243 \times 10^{-3} \cdot X_{16} \quad (2)$$

Table 3. Model summary.

R	R ²	Adjust R ²	Error in Standard Estimation	F	Sig.
0.966	0.933	0.927	1.448	173.49	0.00

Table 4. Model coefficient.

Independent Variable	Non-Standardized Coefficient		Standardized Coefficient	t	Sig.
	B	Standard Error			
Constant	38.840	12.118		3.205	0.002
X ₁	0.106	0.019	0.130	5.594	0.000
X ₂	−0.012	0.004	−0.070	−2.972	0.003
X ₃	−1.491	1.028	−0.035	−1.451	0.148
X ₄	2.355	1.141	0.058	2.064	0.040
X ₅	0.0001	0.006	0.0004	−0.019	0.985
X ₆	1.205	0.966	0.031	1.247	0.214
X ₇	14.302	6.362	0.047	2.248	0.026
X ₈	−1.762	0.051	−1.024	−34.670	0.000
X ₉	15.221	1.039	0.371	14.644	0.000
X ₁₀	−0.610	0.141	−0.094	−4.319	0.000
X ₁₁	0.085	0.080	0.026	1.059	0.291
X ₁₂	0.748	0.325	0.102	2.301	0.022
X ₁₃	−0.011	0.195	−0.002	−0.055	0.956
X ₁₄	0.001	0.001	0.095	2.598	0.010
X ₁₅	−0.015	0.003	−0.192	−4.360	0.000
X ₁₆	0.003	0.002	0.059	1.518	0.131

The model is used to forecast the production data of 50 heats in the test set, and the FeO content in the slag predicted by the regression model is compared with the actual value. The results are shown in Figures 3 and 4.

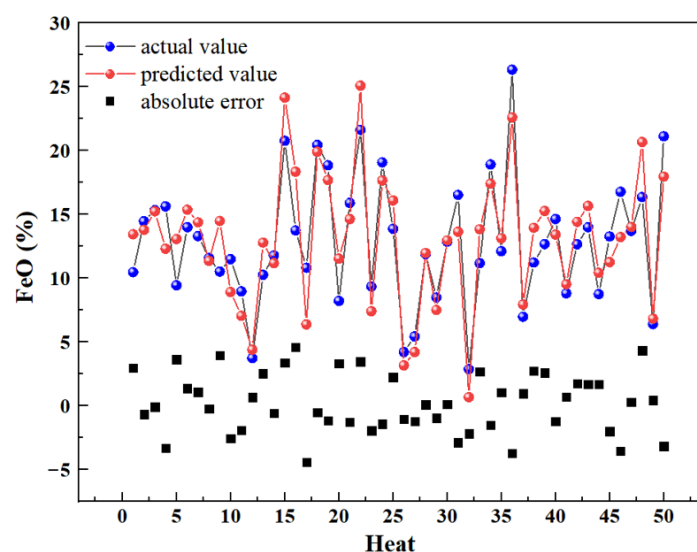


Figure 3. Comparison of actual FeO values and predicted FeO values based on MLR.

Figure 3 shows the comparison between the predicted value of the slag FeO content based on the multiple linear regression model and the actual value. It can be seen from Figure 3 that the multiple linear regression model can better predict the FeO content of slag to a certain extent, but there is a certain deviation from the actual value. According to statistics, the average absolute error of 50 heats of test samples is 1.958%, but the deviation of some heats is large, and the absolute error reaches about 5%, indicating that the stability of the model is not good enough. In order to better reflect the accuracy of the multiple linear regression prediction model, the error distribution histogram between the predicted value of slag FeO content and the actual value of the multiple linear regression model is established, as shown in Figure 4. It can be seen from Figure 4 that the model prediction error range is mainly within $\pm 3.0\%$. When the prediction error range is within $\pm 3.0\%$, the

model prediction hit rate is 76%; when the prediction error is within $\pm 2.0\%$, the hit rate of the model prediction is 56%; and when the prediction error is within $\pm 1.0\%$, the hit rate of the model prediction is only 26%.

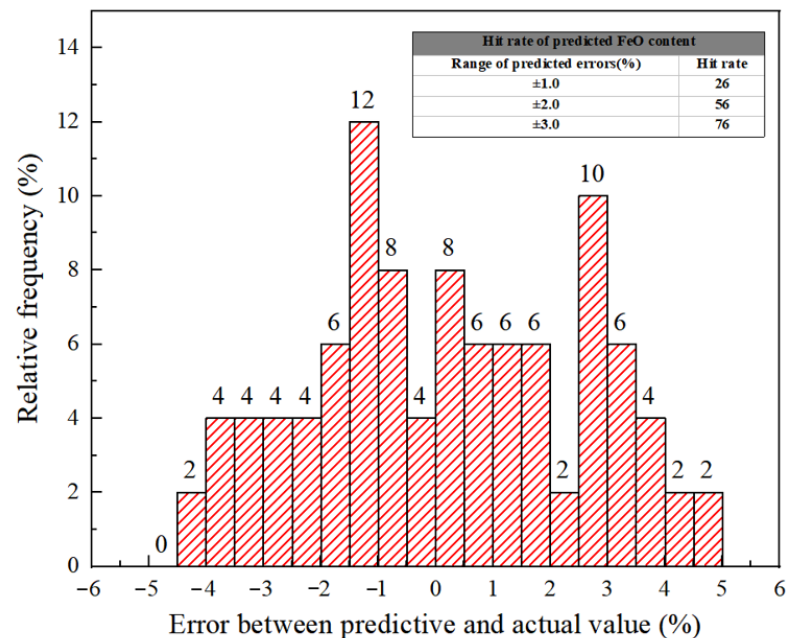


Figure 4. Error distribution of MLR predicted model.

It can be seen from the results of the multiple linear regression prediction model that the effect of the model is not ideal, the model hit rate is low and the stability is not high, and the guidance value for actual production is limited. The reason is that the multiple linear regression model reflects the linear relationship between the input variables and the output variables, but in the converter production process, there are complex physical and chemical reactions, heat and mass transfer and multiphase flow characteristics. It is difficult to simply describe the relationship between the slag FeO content and various factors with a mathematical expression. Therefore, the prediction accuracy of the regression model is affected to some extent. It is necessary to explore a more reasonable method to effectively predict the FeO content of slag with the help of artificial intelligence and statistics technology.

4. Prediction Model of FeO in Slag Based on BP Neural Network

Due to the short blowing time of dephosphorization converter, low smelting temperature and different slagging state of raw and auxiliary materials, it is difficult to effectively predict the FeO content of slag through mechanism model [17]. Artificial neural network has good nonlinear approximation ability, flexible and effective learning mode, fully distributed storage structure and strong fault tolerance [18]. Therefore, using neural network to deal with the problem of nonlinear dynamic system can overcome the weakness of regression model and achieve better prediction results. In this section, the good generalization ability of neural network to complex nonlinear models is used to reflect the nonlinear relationship between the slag FeO content of converter bottom-blowing O_2 -CaO process and various influencing factors, so as to achieve accurate prediction of the slag FeO content.

4.1. Introduction to BP Neural Network

The BP neural network is a multilayer feedforward neural network with error back-propagation. Any nonlinear mapping from input to output can be realized. The structure of multilevel feedforward network based on the BP algorithm is shown in Figure 5. The BP neural network consists of an input layer, an output layer and one or more hidden layers.

Process of BP network training: The network initializes a group of connection weights and thresholds, obtains the output results through the network forward propagation and then compares them with the expected values to obtain the training error. If the error does not reach the expected minimum value, the network backpropagation is started, and the error is reduced by correcting the connection weight and threshold value. The forward propagation output calculation and the backpropagation link weight and threshold correction are carried out in turn until the error between the realized output value and the expected value meets the requirements.

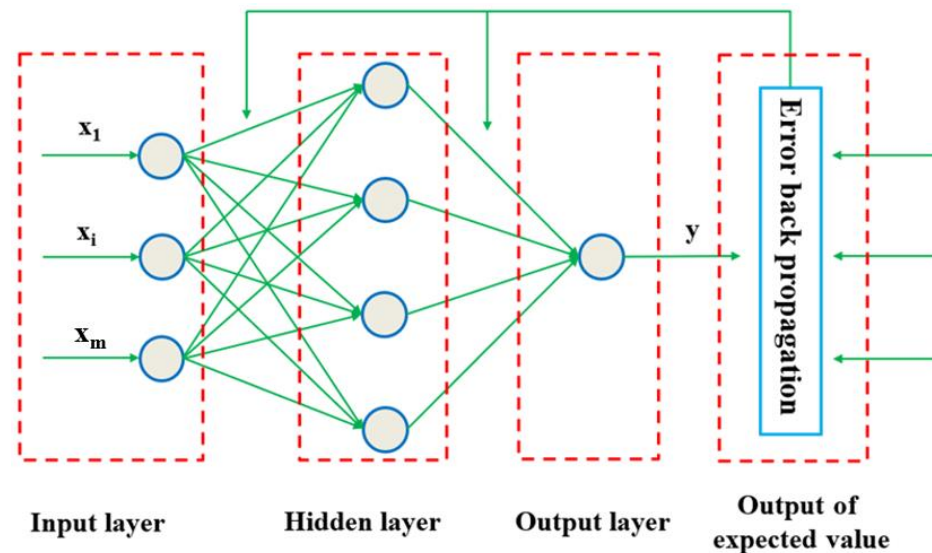


Figure 5. Schematic diagram of BP neural network structure.

4.2. Establishment of BP Neural Network Prediction Model

The BP neural network model in this paper adopts a three-layer structure (one input layer, one output layer and one hidden layer). The model building process is shown in Figure 6. The 16 variables shown in Table 2 are the input variables of this model, and the slag FeO content is the output variable.

On the basis of determining the basic structure of the BP neural network, 217 heats of data in the above section are used to train the established BP neural network model, and the remaining 50 heats of data are used as test sets to verify the trained BP neural network model. Through a continuous comparison between the predicted value and the actual value, the BP neural network with the highest prediction accuracy is retained. In this paper, the Levenberg–Marquardt optimization algorithm is used to train data. Normalize the input and output of the training group with the mapminmax function to obtain the input and output in the $[-1, 1]$ interval. Then normalize the input of the test group and reverse normalize the predicted output. The difference between the predicted output and the actual output is an error. The BP neural network model has the highest prediction accuracy when using the basic parameters given in Table 5.

4.3. Prediction Results and Analysis of BP Neural Network Model

The correlation results of the model training set and test set are shown in Figure 7. Training: $R = 0.98659$. Test: $R = 0.94423$. All R values are greater than 0.9, indicating that the model input variables and output variables are closely related.

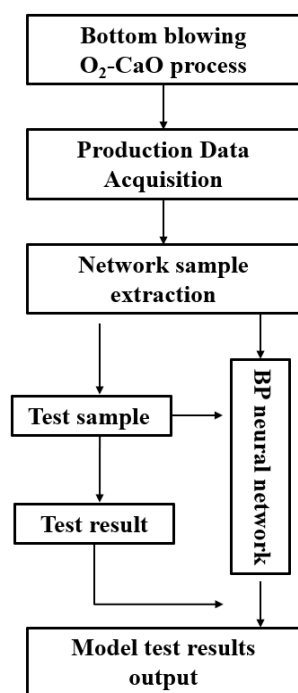


Figure 6. Establishment process of BP neural network model.

Table 5. Fundamental parameters of BP neural network.

Dependent Variable	Fundamental Parameters	Values
y	Nodes of input layer	16
	Number of hidden layers	1
	Nodes of hidden layer	14
	Input layer activation function	Sigmoid
	Nodes of output layer	1
	Data division	random
	Training function	Trainlm
	Learning rate	0.001

Figure 8 shows the comparison between the predicted value of slag FeO content based on the BP neural network model and the actual value. It can be seen from Figure 8 that the predicted value of the BP neural network model is close to the actual value. According to statistics, the average absolute error of 50 heats of test samples is 1.631%, which is 0.3% lower than that of the multiple linear regression prediction model. However, the deviation of some heats is large, and the absolute error reaches about 4.1%, indicating that the stability of the model is still not good enough. In order to better reflect the accuracy of BP neural network prediction model, the error distribution histogram between the predicted value and the actual value of slag FeO content is established, as shown in Figure 9. It can be seen from Figure 9 that when the prediction error range is $\pm 3.0\%$, the model prediction hit rate is 84%; when the prediction error is within $\pm 2.0\%$, the hit rate of the model prediction is 68%; and when the prediction error is within $\pm 1.0\%$, the model prediction hit rate is 38%. It can be seen that, compared with the multiple linear regression model, the BP neural network model has significantly improved the prediction accuracy and stability.

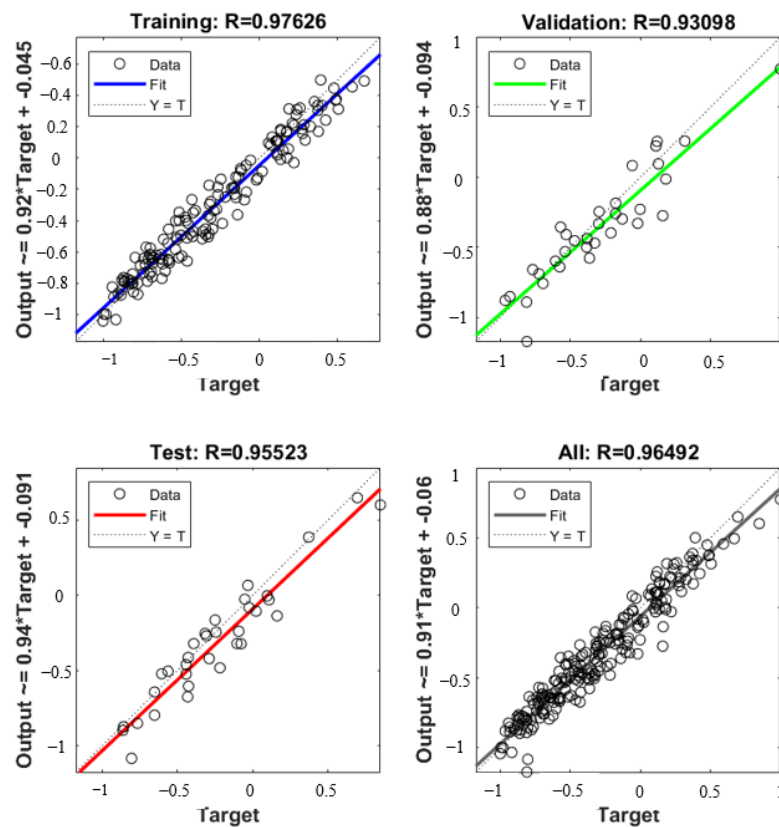


Figure 7. Correlation between training set and test set of BP neural network model.

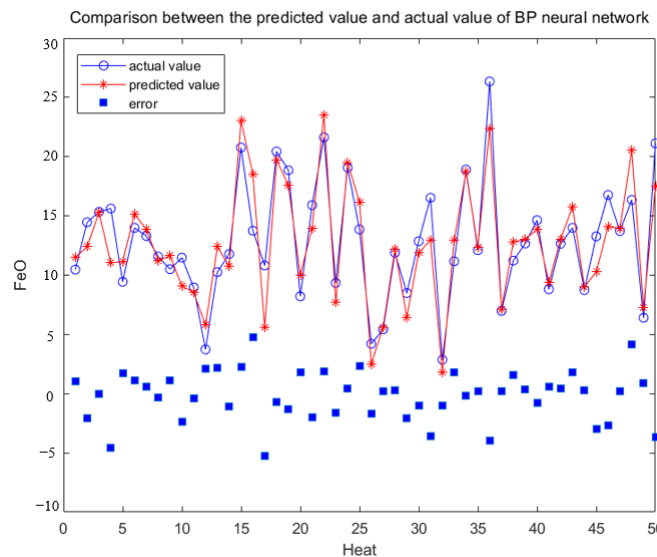


Figure 8. Comparison of predicted and actual FeO content of BP neural network.

Although the predicted value of the FeO content in slag by the BP neural network model is very close to the actual value in some points, there are some points with large errors, especially when the predicted error is 1.0%, and the hit rate is only 38%, making it difficult to meet the conditions of industrial application. It shows that the BP neural network prediction model can be further optimized and improved. In order to meet the actual production requirements and further improve the prediction accuracy of the FeO content in slag, this paper attempts to improve the BP neural network model by applying the principal component analysis and establishing a PCA-BP combined neural network prediction model.

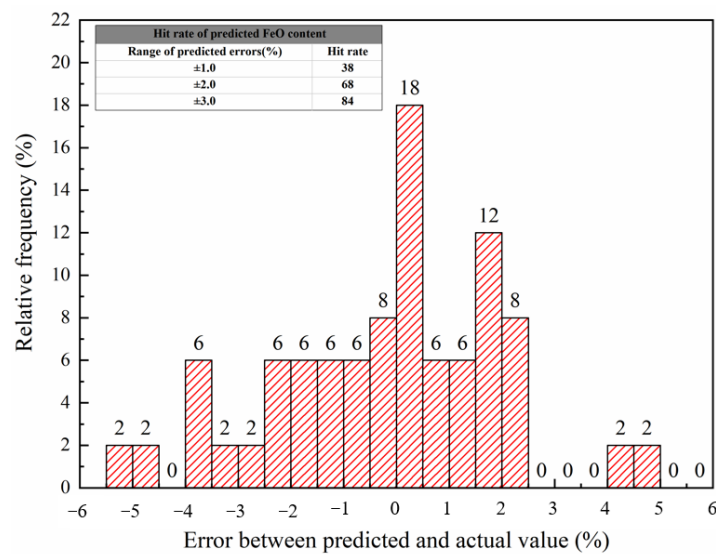


Figure 9. Error distribution of BP neural network predicted model.

5. Prediction Model of FeO in Slag Based on PCA-BP Combined Neural Network

The principal component analysis (PCA) is a mathematical multivariate statistical analysis method that is used to reduce the dimensions of data [19,20]. The basic idea is to replace the variables X_1, X_2, \dots, X_n with a group of unrelated comprehensive variables, Y_1, Y_2, \dots, Y_m ($m < n$), with fewer digits and retain as much internal information as possible in the original variable data set, so as to reduce the dimension of the multivariable system into an independent variable system. As there are many parameters that affect the slag composition in the converter production process, and the data are highly correlated, in order to improve the prediction accuracy of the BP neural network on the slag FeO content, the principal component analysis of the selected 16 independent variables is carried out, and then the PCA-BP composite neural network prediction model is established.

5.1. Mathematical Model of Principal Component Analysis

A sample data matrix with k samples and n variables X_1, X_2, \dots, X_n can be expressed as Equation (3):

$$X = \begin{pmatrix} x_{11} & \dots & x_{1n} \\ \vdots & \ddots & \vdots \\ x_{k1} & \dots & x_{kn} \end{pmatrix} = (X_1, \dots, X_n), \text{ where, } X_i = \begin{bmatrix} x_{1i} \\ x_{2i} \\ \dots \\ x_{ki} \end{bmatrix}, i = 1, 2, 3, \dots, n \quad (3)$$

m new variables are obtained by the principal component analysis, and their expressions are ($m < n$):

$$\begin{cases} F_1 = a_{11}X_1 + a_{12}X_2 + \dots + a_{1n}X_n \\ F_2 = a_{21}X_1 + a_{22}X_2 + \dots + a_{2n}X_n \\ \dots \dots \dots \\ F_m = a_{m1}X_1 + a_{m2}X_2 + \dots + a_{mn}X_n \end{cases} \quad (4)$$

The following conditions shall be met:

- (1) $a_{i1}^2 + a_{i2}^2 + \dots + a_{in}^2 = 1, i = 1, 2, \dots, m;$
- (2) F_i, F_j is uncorrelated;
- (3) $Var(F_1) > Var(F_2) > \dots > Var(F_m).$

The first principal component is F_1 . The second principal component is F_2 . By analogy, the principal component coefficient is a_{ij} . It can also be expressed as $F = AX$, which means that A is the coefficient matrix of the main component.

$$A = \begin{pmatrix} a_{11} & \cdots & a_{1n} \\ \vdots & \ddots & \vdots \\ a_{m1} & \cdots & a_{mn} \end{pmatrix} = \begin{bmatrix} a_1 \\ a_2 \\ \cdots \\ a_n \end{bmatrix} \quad (5)$$

5.2. Establishment of PCA-BP Combined Neural Network Model

According to the above analysis, the principal component analysis can effectively reduce the dimension of input vectors, eliminate the correlation between input vectors and retain most of the information in input vectors. In this paper, SPSS (IBM Corporation, New York, NY, USA) is used for the principal component analysis of input variables. The input variables are 16 factors of the production data of 217 heats of the training set introduced in the Section 2. Thus, a 217×16 sample data matrix is obtained.

According to the actual production data, the principal component analysis of 16 factors in the converter bottom-blowing O_2 -CaO process is carried out. The cumulative contribution rate of the principal components is obtained by using SPSSPRO software, as shown in Table 6. According to the cumulative contribution rate, the number of principal components to be extracted is determined. Generally speaking, the cumulative contribution rate is required to reach more than 90%, so that most of the information of the original data can be preserved.

Table 6. Total variance interpretation.

Component	Initial Eigenvalues		
	Total	% of Variance	Cumulative %
1	3.854	22.400	22.400
2	2.209	13.807	36.207
3	1.885	11.782	47.989
4	1.519	9.494	57.483
5	1.259	7.870	65.353
6	1.028	6.425	71.778
7	0.897	5.605	77.383
8	0.808	5.050	82.433
9	0.749	4.679	87.112
10	0.510	3.185	90.297
11	0.475	2.970	93.267
12	0.367	2.292	95.559
13	0.314	1.960	97.519
14	0.193	1.204	98.732
15	0.114	0.713	99.436
16	0.090	0.564	100.000

As can be seen from Table 6, the cumulative contribution rate of the first 10 principal components reaches 90.514%. This means that, as long as the first 10 principal components are selected, most of the information of the original matrix can be saved. Therefore, the number of principal components selected in this paper is 10. The formula is as shown in Equation (6):

$$\begin{aligned}
F_1 &= 0.049 \cdot X_1 + 0.069 \cdot X_2 - 0.039 \cdot X_3 - 0.06 \cdot X_4 - 0.053 \cdot X_5 - 0.024 \cdot X_6 - 0.021 \cdot X_7 + 0.146 \cdot X_8 \\
&\quad + 0.126 \cdot X_9 - 0.011 \cdot X_{10} + 0.05 \cdot X_{11} + 0.207 \cdot X_{12} - 0.218 \cdot X_{13} - 0.173 \cdot X_{14} + 0.203 \cdot X_{15} - 0.235 \cdot X_{16} \\
F_2 &= 0.247 \cdot X_1 + 0.159 \cdot X_2 + 0.134 \cdot X_3 + 0.218 \cdot X_4 - 0.022 \cdot X_5 - 0.024 \cdot X_6 + 0.001 \cdot X_7 + 0.051 \cdot X_8 \\
&\quad + 0.002 \cdot X_9 + 0.275 \cdot X_{10} + 0.328 \cdot X_{11} - 0.140 \cdot X_{12} + 0.135 \cdot X_{13} - 0.172 \cdot X_{14} - 0.080 \cdot X_{15} - 0.051 \cdot X_{16} \\
F_3 &= -0.126 \cdot X_1 - 0.179 \cdot X_2 + 0.253 \cdot X_3 + 0.325 \cdot X_4 + 0.13 \cdot X_5 + 0.201 \cdot X_6 + 0.179 \cdot X_7 + 0.071 \cdot X_8 \\
&\quad - 0.108 \cdot X_9 + 0.023 \cdot X_{10} + 0.037 \cdot X_{11} + 0.246 \cdot X_{12} - 0.024 \cdot X_{13} + 0.257 \cdot X_{14} + 0.278 \cdot X_{15} - 0.012 \cdot X_{16} \\
F_4 &= -0.083 \cdot X_1 + 0.085 \cdot X_2 - 0.198 \cdot X_3 + 0.081 \cdot X_4 + 0.311 \cdot X_5 - 0.222 \cdot X_6 + 0.318 \cdot X_7 + 0.417 \cdot X_8 \\
&\quad + 0.337 \cdot X_9 + 0.139 \cdot X_{10} - 0.049 \cdot X_{11} - 0.039 \cdot X_{12} + 0.171 \cdot X_{13} + 0.03 \cdot X_{14} - 0.041 \cdot X_{15} + 0.101 \cdot X_{16} \\
F_5 &= -0.23 \cdot X_1 + 0.29 \cdot X_2 + 0.476 \cdot X_3 - 0.116 \cdot X_4 + 0.03 \cdot X_5 + 0.116 \cdot X_6 - 0.394 \cdot X_7 + 0.158 \cdot X_8 \\
&\quad + 0.321 \cdot X_9 + 0.128 \cdot X_{10} - 0.152 \cdot X_{11} + 0.061 \cdot X_{12} - 0.128 \cdot X_{13} + 0.1 \cdot X_{14} - 0.115 \cdot X_{15} + 0.191 \cdot X_{16} \\
F_6 &= 0.399 \cdot X_1 - 0.591 \cdot X_2 - 0.13 \cdot X_3 - 0.19 \cdot X_4 + 0.025 \cdot X_5 + 0.335 \cdot X_6 - 0.255 \cdot X_7 + 0.257 \cdot X_8 \\
&\quad + 0.126 \cdot X_9 + 0.245 \cdot X_{10} - 0.266 \cdot X_{11} - 0.024 \cdot X_{12} + 0.072 \cdot X_{13} + 0.048 \cdot X_{14} + 0.037 \cdot X_{15} + 0.107 \cdot X_{16} \\
F_7 &= 0.09 \cdot X_1 + 0.207 \cdot X_2 - 0.055 \cdot X_3 - 0.281 \cdot X_4 + 0.864 \cdot X_5 + 0.248 \cdot X_6 - 0.034 \cdot X_7 - 0.138 \cdot X_8 \\
&\quad - 0.314 \cdot X_9 + 0.02 \cdot X_{10} - 0.031 \cdot X_{11} - 0.0158 \cdot X_{12} - 0.196 \cdot X_{13} - 0.1 \cdot X_{14} - 0.008 \cdot X_{15} - 0.068 \cdot X_{16} \\
F_8 &= 0.296 \cdot X_1 + 0.116 \cdot X_2 - 0.012 \cdot X_3 + 0.116 \cdot X_4 + 0.099 \cdot X_5 - 0.673 \cdot X_6 - 0.44 \cdot X_7 + 0.018 \cdot X_8 \\
&\quad - 0.291 \cdot X_9 + 0.371 \cdot X_{10} + 0.012 \cdot X_{11} + 0.026 \cdot X_{12} + 0.035 \cdot X_{13} + 0.418 \cdot X_{14} + 0.252 \cdot X_{15} - 0.05 \cdot X_{16} \\
F_9 &= 0.171 \cdot X_1 - 0.234 \cdot X_2 + 0.054 \cdot X_3 + 0.182 \cdot X_4 + 0.308 \cdot X_5 - 0.119 \cdot X_6 - 0.414 \cdot X_7 + 0.105 \cdot X_8 \\
&\quad + 0.288 \cdot X_9 - 0.747 \cdot X_{10} + 0.511 \cdot X_{11} - 0.066 \cdot X_{12} + 0.088 \cdot X_{13} + 0.066 \cdot X_{14} - 0.039 \cdot X_{15} + 0.065 \cdot X_{16} \\
F_{10} &= 0.161 \cdot X_1 + 0.527 \cdot X_2 - 0.191 \cdot X_3 + 0.371 \cdot X_4 - 0.135 \cdot X_5 + 0.266 \cdot X_6 - 0.26 \cdot X_7 + 0.515 \cdot X_8 \\
&\quad - 0.475 \cdot X_9 - 0.486 \cdot X_{10} - 0.578 \cdot X_{11} + 0.096 \cdot X_{12} + 0.433 \cdot X_{13} - 0.2 \cdot X_{14} + 0.135 \cdot X_{15} + 0.095 \cdot X_{16}
\end{aligned} \tag{6}$$

The 217 heats production data of the training set are brought into the above 10 principal component formulas to obtain 217 sets of new input variables. The BP neural network model is trained with 217 sets of new input scalars. The remaining 50 heats production data are used as the test set to verify the trained BP neural network model. Similarly, the Levenberg–Marquardt algorithm is used to optimize the training data. Normalize the input and output of the training group with the mapminmax function to obtain the input and output in the $[-1, 1]$ interval. Then normalize the input of the test group and reverse normalize the predicted output. The PCA-BP neural network model has the highest prediction accuracy when using the basic parameters given in Table 7.

Table 7. Fundamental parameters of PCA-BP neural network.

Dependent Variable	Fundamental Parameters	Values
Y	Nodes of input layer	10
	Number of hidden layers	1
	Nodes of hidden layer	14
	Input layer activation function	Sigmoid
	Nodes of output layer	1
	Data division	random
	Training function	trainlm
	Learning rate	0.000001

5.3. Prediction Results and Analysis of PCA-BP Combined Neural Network Model

The PCA-BP neural network is used to predict and analyze the FeO content in the slag of the bottom-blowing O_2 -CaO process. The correlation results between the model training set and the test set are shown in Figure 10. Training: $R = 0.91104$. Test: $R = 0.9304$. All R values are greater than 0.9, indicating that the input variables and output variables of the model are closely related.

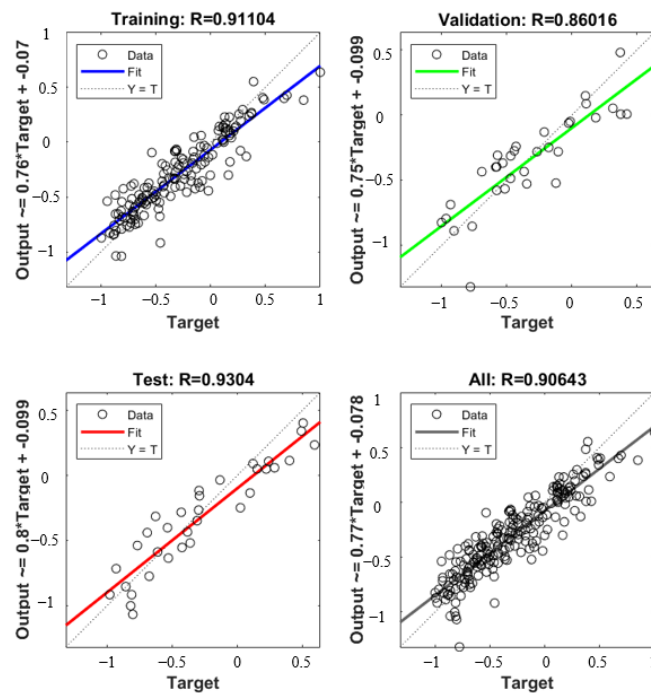


Figure 10. Correlation between training set and test set of PCA-BP neural network model.

Figure 11 shows the comparison between the predicted value of slag FeO content based on PCA-BP combined neural network model and the actual value. It can be seen from Figure 11 that the predicted value of the PCA-BP combined neural network model is very consistent with the actual value, and the change trend is basically consistent. According to statistics, the average absolute error of 50 heat test samples is 1.178%, which is 0.78% lower than that of the multiple linear regression prediction model and 0.453% lower than that of the BP neural network prediction model. In order to better reflect the accuracy of the PCA-BP neural network prediction model, the error distribution histogram between the predicted value and the actual value of the slag FeO content of the PCA-BP neural network model is established, as shown in Figure 12. It can be seen from Figure 12 that when the prediction error range is $\pm 3.0\%$, the model prediction hit rate is 96%; when the prediction error is within $\pm 2.0\%$, the model prediction hit rate is 78%; and when the prediction error is within $\pm 1.0\%$, the model prediction hit rate is 54%. It can be seen that the PCA-BP neural network prediction model has the highest prediction accuracy and has important reference value for actual production.

Table 8 visually compares the prediction effects of three models: multiple linear regression model, BP neural network model and PCA-BP combined neural network model. It can be seen from Table 8 that the PCA-BP combined neural network model has the smallest prediction error and the highest hit rate. The PCA-BP combined neural network model is obviously superior to the MLR model and BP neural network model in both prediction accuracy and stability, and this model has a greater practical application value.

Table 8. Comparison of accuracy and error of three prediction models.

Model	MLR	BP	PCA-BP
$\pm 1.0\%$	26%	38%	54%
$\pm 2.0\%$	56%	68%	78%
$\pm 3.0\%$	76%	84%	96%
Mean absolute error	1.958%	1.631%	1.178%

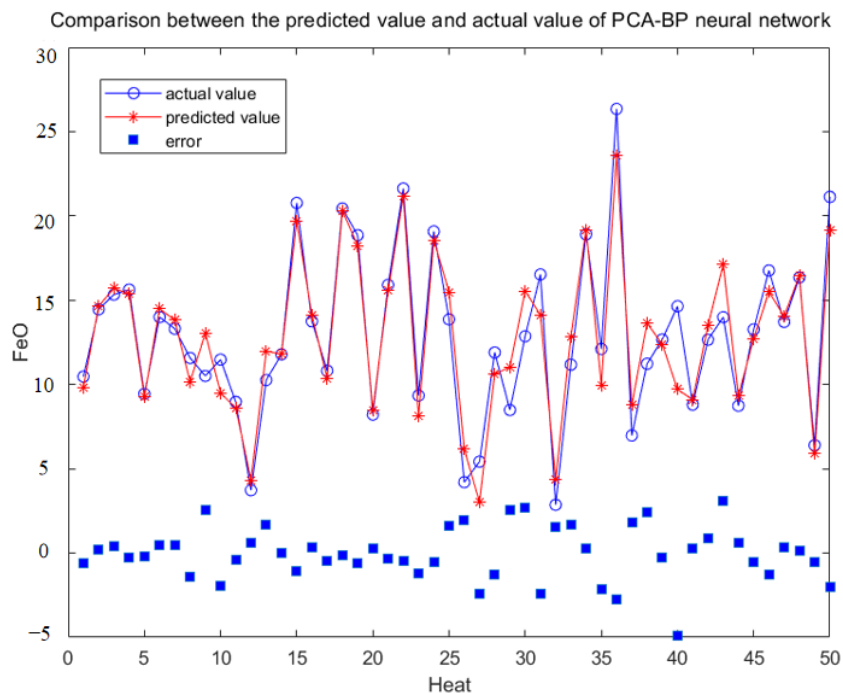


Figure 11. Comparison of predicted and actual FeO content of PCA-BP neural network.

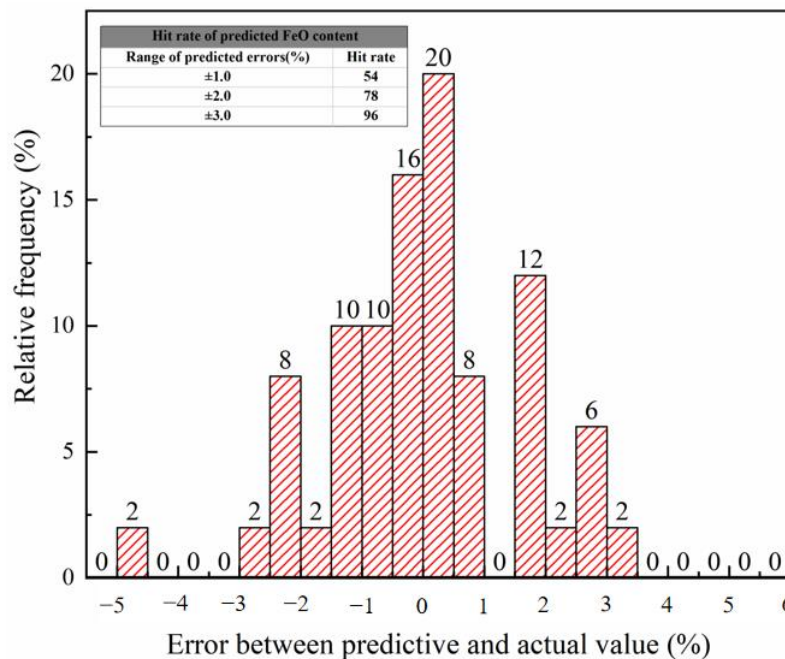


Figure 12. Error distribution of PCA-BP neural network predictive model.

6. Summary and Conclusions

In order to accurately predict the FeO content of slag in the bottom-blowing O₂-CaO process of dephosphorization converter and provide the basis for optimizing the operation system of the bottom-blowing O₂-CaO process, this paper established a multiple linear regression model, BP neural network model and PCA-BP combined neural network model to predict the FeO content of slag. The main conclusions of this paper are as follows:

- (1) By establishing the multiple linear regression model, the relationship between FeO content in slag and various influencing factors is obtained:

$$Y = -3.884 \times 10 + 1.061 \times 10^{-1} \cdot X_1 - 1.245 \times 10^{-2} \cdot X_2 - 1.491 \cdot X_3 + 2.355 \cdot X_4 - 1.055 \times 10^{-4} \cdot X_5 + 1.205 \cdot X_6 + 1.430 \times 10 \cdot X_7 - 1.726 \cdot X_8 + 1.522 \times 10 \cdot X_9 - 6.099 \times 10 \cdot X_{10} + 8.491 \times 10^{-2} \cdot X_{11} + 7.477 \times 10^{-1} \cdot X_{12} - 1.072 \times 10^{-2} \cdot X_{13} + 1.425 \times 10^{-3} \cdot X_{14} - 1.453 \times 10^{-2} \cdot X_{15} + 3.243 \times 10^{-3} \cdot X_{16}$$

However, the average absolute error of the model is 1.958%, and the hit rate of the model in the high-precision range is low.

- (2) The average absolute error of the BP neural network prediction model is 1.631%, which is 0.3% lower than that of the multiple linear regression prediction model. When the prediction error range is 3.0%, the prediction hit rate of the model is 84%, and when the prediction error range is 2.0%, the prediction hit rate of the model is 68%. Compared with the multiple linear regression model, the BP neural network model has obviously improved prediction accuracy and stability.
- (3) The average absolute error of the PCA-BP combined neural network model is 1.178%, which is 0.78% lower than that of the multiple linear regression prediction model and 0.453% lower than that of the BP neural network prediction model. When the prediction error is within $\pm 3.0\%$, the hit rate of the model prediction is 96%, and when the prediction error is within $\pm 2.0\%$, the model prediction hit rate is 78%. The PCA-BP neural network prediction model has the highest prediction accuracy and has important reference value for actual production.

Author Contributions: Conceptualization, X.R.; methodology, X.R.; soft-ware, C.W.; validation, G.W.; formal analysis, C.F.; investigation, X.R.; data curation, C.W.; writing-original draft preparation, X.R.; writing-reviewand editing, X.R.; visualization, K.D.; supervision, K.D.; funding acquisition, R.Z. All authors have read and agreed to the published version of the manuscript.

Funding: This work was supported by the National Natural Science Foundation of China (No. 51974024, No. 52074024 and No. 52004023) and the China Baowu Low Carbon Metallurgy Innovation Foundation—BWLCF202108.

Institutional Review Board Statement: Not applicable.

Informed Consent Statement: Not applicable.

Data Availability Statement: Not applicable.

Conflicts of Interest: The authors declare no conflict of interest.

References

- Ye, G.; Yang, J.; Zhang, R.; Yang, W.; Sun, H. Behavior of phosphorus enrichment in dephosphorization slag at low temperature and low basicity. *Int. J. Min. Met. Mater.* **2021**, *28*, 66. [\[CrossRef\]](#)
- Lee, C.M.; Fruehan, R.J. Phosphorus equilibrium between hot metal and slag. *Ironmak Steelmak.* **2005**, *32*, 503. [\[CrossRef\]](#)
- Tian, Z.; Li, B.; Zhang, X.; Jiang, Z.J. Double slag operation dephosphorization in BOF for producing low phosphorus steel. *Iron Steel Res. Int.* **2009**, *16*, 6. [\[CrossRef\]](#)
- Hamano, T.; Horibe, M.; Ito, K. The dissolution rate of solid lime into molten slag used for hot-metal dephosphorization. *ISIJ Int.* **2004**, *44*, 263. [\[CrossRef\]](#)
- Deng, T.; Gran, J.; Sichen, D. Dissolution of Lime in Synthetic 'FeO'-SiO₂ and CaO-'FeO'-SiO₂ Slags. *Steel Res. Int.* **2010**, *81*, 347. [\[CrossRef\]](#)
- Zhou, Y.; Zhu, R.; Hu, S.; Li, W. Study on metallurgical characteristics of the bottom-blown O₂-CaO converter. *Ironmak Steelmak.* **2021**, *48*, 142. [\[CrossRef\]](#)
- Matsui, A.; Nabeshima, S.; Matsuno, H.; Kishimoto, Y. Kinetics behavior of iron oxide formation under the condition of oxygen top blowing for dephosphorization of hot metal in the basic oxygen furnace. *Tetsu Hagane* **2009**, *95*, 207. [\[CrossRef\]](#)
- Zhao, Z.C.; Sun, Y.H.; Luo, Y.H.; Zhao, C.L. The dynamic prediction model of FeO mass fraction in slag in 300 t top-bottom combined blowing converter. *Steelmaking* **2015**, *31*, 13.

9. Gao, M.; Gao, J.T.; Zhang, Y.L.; Yang, S.F. Evaluation and Modeling of Scrap Utilization in the Steelmaking Process. *JOM* **2021**, *73*, 712. [[CrossRef](#)]
10. Wang, Z.; Chang, J.; Ju, Q.P.; Xie, F.M.; Wang, B.; Li, H.W. Prediction model of end-point manganese content for BOF steelmaking process. *ISIJ Int.* **2012**, *52*, 1585. [[CrossRef](#)]
11. He, F.; Zhang, L.J. Prediction model of end-point phosphorus content in BOF steelmaking process based on PCA and BP neural network. *Process Control.* **2018**, *66*, 51. [[CrossRef](#)]
12. Chen, C.; Wang, N.; Chen, M. Prediction Model of End-point Phosphorus Content in Consteel Electric Furnace Based on PCA-Extra Tree Model. *ISIJ Int.* **2021**, *61*, 1908. [[CrossRef](#)]
13. Sasmita, S.; Sahoo, J. Groundwater-level prediction using multiple linear regression and artificial neural network techniques: A comparative assessment. *Hydrogeol. J.* **2013**, *21*, 1865.
14. Hsu, C.C.; Lin, J.; Chao, C.K. Comparison of multiple linear regression and artificial neural network in developing the objective functions of the orthopaedic screws. *Comput. Methods Programs Biomed.* **2011**, *104*, 341. [[CrossRef](#)] [[PubMed](#)]
15. Piro, N.S.; Mohammed, A.S.; Hamed, S.M. Evaluate and predict the resist electric current and compressive strength of concrete modified with GGBS and steelmaking slag using mathematical models. *J. Sustain. Metall.* **2023**, *9*, 194. [[CrossRef](#)]
16. Bucur, A.; Dobrotă, G.; Oprean-Stan, C.; Tănăsescu, C. Economic and qualitative determinants of the world steel production. *Metals* **2017**, *7*, 163. [[CrossRef](#)]
17. Su, X.W.; Cui, H.; Zhang, B.L.; Liu, Y.Q.; Luo, L. FeO prediction model of dephosphorization slag in converter for dephosphorization. *JCQU-E* **2018**, *41*, 56.
18. Hunt, K.J.; Sbarbaro, D. Adaptive filtering and neural networks for realisation of internal model control. *IEE Proc.-D Control Theor.* **1991**, *138*, 431. [[CrossRef](#)]
19. Abdi, H.; Williams, L.J. Principal component analysis. *WIREs Comput. Stat.* **2010**, *2*, 433. [[CrossRef](#)]
20. Liu, Z.; Cheng, S.S.; Liu, P.B. Prediction model of BOF end-point P and O contents based on PCA-GA-BP neural network. *High Temp. Mater. Process.* **2022**, *41*, 505. [[CrossRef](#)]

Disclaimer/Publisher's Note: The statements, opinions and data contained in all publications are solely those of the individual author(s) and contributor(s) and not of MDPI and/or the editor(s). MDPI and/or the editor(s) disclaim responsibility for any injury to people or property resulting from any ideas, methods, instructions or products referred to in the content.